Two-Phase Steam–Water Flow Through *Y*-Junctions

J. Kubie† and H. S. Oates

An investigation has been made of steam–water flow in vertical coplanar *Y*-junctions which are used, for example, in the condensate carrying pipework downstream of direct contact heat exchangers. The steam–water flow is stratified in the sloping limbs approaching the junction and this paper examines problems associated with the flooding of the junction. It is shown that at low water flowrates water falls freely through the junction, but as the water flowrate increases a condition is reached when the water starts to pile at the junction and the junction is said to be flooded. Further increase in the water flowrate causes the water level to rise within the sloping limbs approaching the junction. A simple analytical model is developed which describes reasonably well the flow phenomena observed.

NOTATION

A_2	$A_{2w}/\pi R^2$, dimensionless cross-sectional area
A_{1w}	cross-sectional area occupied by water at station 1
A_{2w}	cross-sectional area occupied by water at station 2
C_d	discharge coefficient
D	force defined by eq. (5)
f	friction factor
g	acceleration due to gravity
G	force defined by eq. (4)
h	head defined by eq. (7)
l	length defined by eq. (14)
l'	length specified in Fig. 7
L	length specified in Fig. 7
M	vertical component of the momentum
p	static pressure
P	pressure force
Q_{wl}	water flowrate in each inclined limb
Q_T^*	total water flowrate at incipient flooding
R	radius of the limbs
V	water velocity
V_c	mean water velocity in the water column
V_{1w}	mean water velocity at station 1
V_{1w}^*	V_{1w} at incipient flooding
V_{2w}	mean water velocity at station 2
α	angle of the velocity to the vertical
α_M	effective angle in eq. (3) for calculating momentum
α_V	effective angle in eq. (10) for calculating flowrate
β	$\cos^2 \alpha_M/\cos^2 \alpha_V$, momentum correction coefficient
ρ_w	water density
θ	angle of the inclined limb to the vertical
τ_w	wall shear

Subscripts

1, 2, c	station in the junction
min	minimum value of a quantity
max	maximum value of a quantity

† Central Electricity Research Laboratories, Leatherhead, Surrey, England. Present address: Engineering Department, CEGB SER, Laud House, London EC1.

Received on 24 July 1979 and accepted for publication on 19 October 1979.

1 INTRODUCTION

This paper is one in a series concerned with the design and performance of pipework carrying liquids under gravity. The importance of proper sizing and layout of the pipework in eliminating adverse flow regimes has been discussed by Simpson (**1**).

This work describes an investigation of two-phase steam–water flow through symmetric *Y*-junctions, as illustrated in Fig. 1. Such a design is of importance since a process vessel may be drained through two outlets which combine in such a fashion. In order to facilitate construction by welding all limbs are usually of the same size. The present authors are mainly interested in drainage of direct contact heat exchangers but the results are general and may be applied to other cases of vapour–liquid gravity flow.

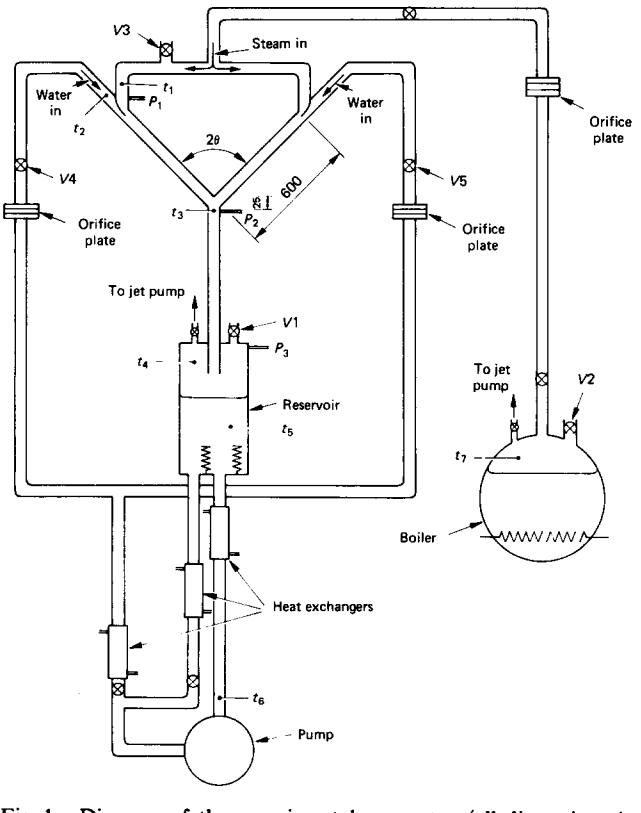

Fig. 1. Diagram of the experimental apparatus (all dimensions in millimetres)

0142/727X/79/1200-0161$2.00

The investigation is restricted to equal flows in both limbs approaching the junction with steam–water flow there being stratified and the water velocity approaching the steady equilibrium value (i.e., the velocity which would be obtained if the inclined limbs were infinitely long). The primary objective of this work is to determine the flooding capacity of the junction, that is, the critical water flowrate above which the water starts piling up at the junction and the influence on flooding of various parameters, such as the angle of the junction and the degree of water subcooling.

A preliminary investigation using an air–water analogue was recently undertaken and certain hydrodynamic processes were identified (**2**). However, an air–water system cannot model change of phase and thus it may differ from a steam–water system which allows for steam flashing.

A comparison of the previous air–water work with the present steam–water work shows that time scales required are considerably longer for the latter investigation. Hence an additional objective of this work is to determine how closely does the air–water modelling approximate to the more time-consuming steam–water modelling.

Experimental and theoretical results are presented in the following sections and it is shown that the flow behaviour in the junction can be explained on the basis of a simple model.

2 EXPERIMENTAL INVESTIGATION

2.1 Apparatus

The diagram of the experimental apparatus is shown in Fig. 1. The *Y*-junctions were constructed from 26 mm bore 'Perspex' tube, the diameter of the tube being large enough for the effect of the surface tension forces to be small. Three junctions with included half-angles of 15°, 30°, and 45° were used with 1300 mm long vertical limb. The vertical limb was discharging into a glass reservoir and its outlet was unobstructed and situated well above the water level there. Water was drawn from the reservoir and supplied to the top of the inclined limbs by a centrifugal pump. Steam was supplied to the top of the inclined limbs from a 15 kW boiler. The water temperature was controlled by five 2 kW kettle elements situated on the bottom of the glass reservoir and by three heat exchangers in the water line. The use of 'Perspex' necessitated the operating temperature to be kept below 60° C, so that the rig was evacuated to low pressures when saturated steam–water conditions were required.

The principal measurements were of the flowrate of water and the temperature and pressure at various points along the test section (as indicated in Fig. 1). The flowrate of water was measured with an orifice plate, the temperature with Cr-Al thermocouples and the pressure with pressure transducers. The flow patterns in the inclined and the vertical limbs were observed visually and when water started to pile up above the junction the length of the inclined limbs completely occupied by water (the water column) was also measured.

2.2 Steam–Water Flow

The steam–water flow constituted the major part of this investigation. The required test conditions were adjusted as follows. The water was allowed to circulate through the test section and was heated to the required temperature when the evacuation of the rig started. The approach of a steam–water condition was characterized by several distinct transitions, such as (1) a 'cracking' noise due to the explosive collapse of steam bubbles entrained at various interfaces became apparent and (2) steam entrainment from condensate impacting on various interfaces dimished and became localized. When saturated steam–water flow over the junction was achieved air extraction rate was decreased and the pressure in the rig was controlled by the heat input into the kettle elements and the boiler.

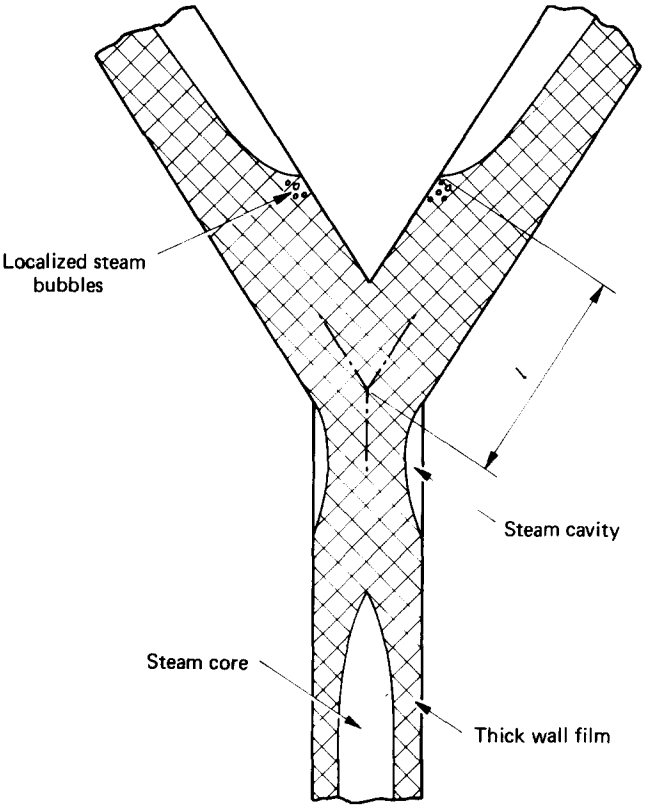

Fig. 2(a). Steam–water flow in a flooded *Y*-junction

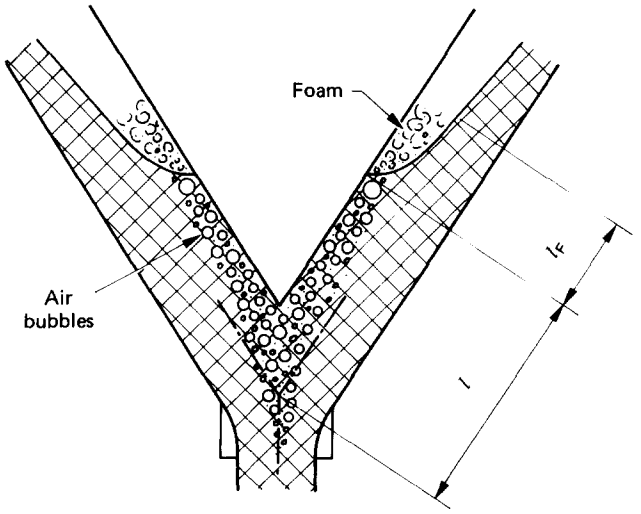

Fig. 2(b). Air–water flow in a flooded *Y*-junction with a short downcomer

Observation of the flow pattern revealed that at low water flowrates the two water streams from the inclined limbs combined at the junction and the water then fell through the vertical limb contacting its walls intermittently. As the water flowrate increased water started to pile up at the junction and eventually water columns were formed in the inclined limbs above the junction. The flow pattern within the vertical limb then changed in that, as shown in Fig. 2(a), the water flowing through the junction reattached to the walls a short distance below the junction, then ran in full pipe flow for a short distance and finally, accelerating under gravity, it divided to run down the walls as a thick annular film with a wavy surface thus forming a central core of (probably) drop laden steam. The water flowrate at which the water started to pile up at the junction was measured.

As the water flowrate was increased further, the length of the water columns in the inclined limbs increased too. This length was well defined and the measurements of the variation of the water column length l with the total water flowrate are plotted for the saturated steam–water flow at 50° C in the three Y-junctions in Fig. 3. (The flooding is indicated by the maximum water flowrate at which l is equal to zero).

To investigate the effect of water subcooling on the effective discharge capacity of the Y-junctions the water was cooled by the operation of the heat exchangers. At the same time the pressure p_1 (in the steam spaces in the inclined limbs above the junction) was kept constant by increasing the power input into the boiler. Thus the water was subcooled with respect to the steam pressure and temperature above the junction. The subcooling pressure was determined by measuring the gauge pressure p_1-p_3.

The change in the effective discharge capacity of the junctions was quantified by setting the length of the water column above the junction at the saturation condition and then increasing the flowrate to keep the level constant as the degree of the water subcooling was being increased. The most comprehensive results were obtained for the 30° Y-junction and they are presented in Fig. 4 which shows that as the degree of the water subcooling increased the apparent discharge capacity of the junction increased too. Similar results were also obtained for the 15° and 45° Y-junctions.

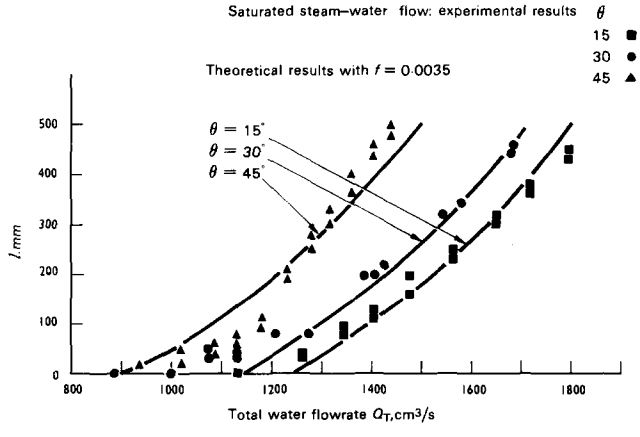

Fig. 3. Flooding of Y-junctions with saturated steam–water flow

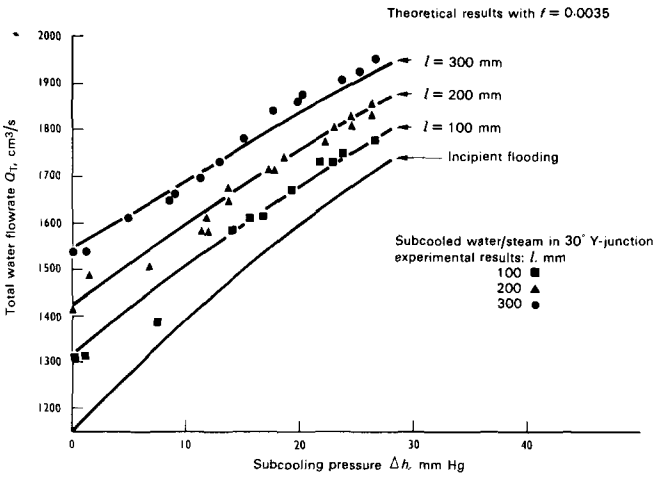

Fig. 4. Flooding of 30° Y-junction with subcooled water–steam flow

2.3 Air–Water Flow

It has been shown previously by Kubie and Gardner (2) that the flooding flowrates for air–water flow in Y-junctions increase with the increasing length of the vertical limb. This is because the weight of the two-phase mixture in the vertical limb creates a suction pressure just below the junction thus helping to accelerate the water through it. In the case of saturated steam–water flow the condensate within the vertical limb cannot exert any 'pull' on the liquid above the junction since the pressure below the junction also tends to the saturation pressure of the condensate. Thus one ought to get nominally similar conditions between saturated steam–water flow and air–water flow by decreasing the length of the vertical limb in the latter case.

This hypothesis was tested by cutting the length of the vertical limb to 15 mm. The saturated steam–water flow was modelled by opening the valves $V3$ and $V1$ (see Fig. 1) so that air could be drawn in and discharged out freely and thus the pressures above and below the junctions were effectively the same. At low water flowrates the junction could discharge all water supplied to it. However, at a certain critical water flowrate the water started to pile up at and above the junction. The major difference between the steam–water and the air–water flow was in the appearance of the water column. The top of the water column was well defined when using steam and water but with air and water there was a considerable amount of foam (high voidage air–water mixture) above the top of the water column and a substantial number of entrained air bubbles below it. Additionally, in contrast to steam–water flow, these bubbles were not localized but propagated throughout the length of the water column (Fig. 2(b)). This meant that some judgement was required to decide about the position of the top of the water column and hence the length of it was subject to an error of up to 20 mm. The level l is plotted against the total water flowrate for the case of all three junctions in Fig. 5.

The flow of steam and subcooled water was modelled with air and water by creating a vacuum in the glass reservoir by closing the valve $V1$ and by evacuation through the reservoir jet pump. As in the steam–water experiments, the length of the water column within the

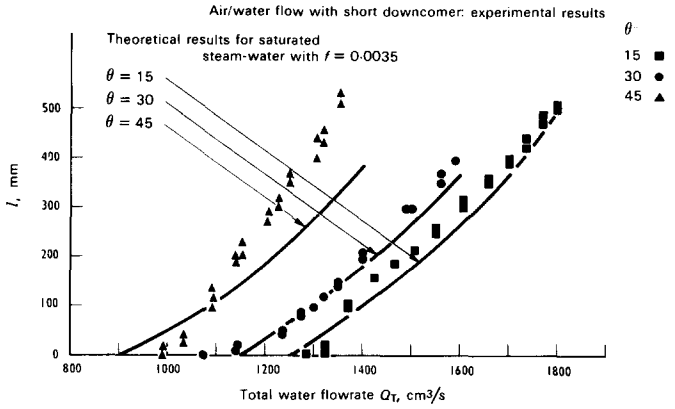

Fig. 5. Flooding of Y-junctions with very short vertical limbs with air–water flow

inclined limbs was set to a required value when the pressure in the reservoir was the same as the ambient pressure p_1. When the pressure in the reservoir decreased the flowrate of water was adjusted so that the length of the water column remained constant. The most comprehensive results were obtained for the 30° Y-junction and they are presented in Fig. 6 which shows that, as with the steam–water flow, the apparent discharge capacity of the Y-junction increases with decreasing pressure below the junction (or increasing pressure difference p_1-p_3). Similar results were also obtained for the 15° and 45° Y-junctions.

3 THEORETICAL ANALYSIS

3.1 General Equations for Steam–Water Flow

The purpose of this section is to develop a general model which can be used for the prediction of flooding and other related phenomena, such as the rise of water in the inclined limbs of Y-junctions.

Referring to Fig. 7, consider the flow of steam and water in a control volume bounded by planes 1 and 2 (inlet and outlet, respectively) and the internal walls of the junction. The distance l' is the length of the inclined limb from the top of the water column to the apex of the junction and L is the distance from the apex of the junction to the inlet into the vertical limb.

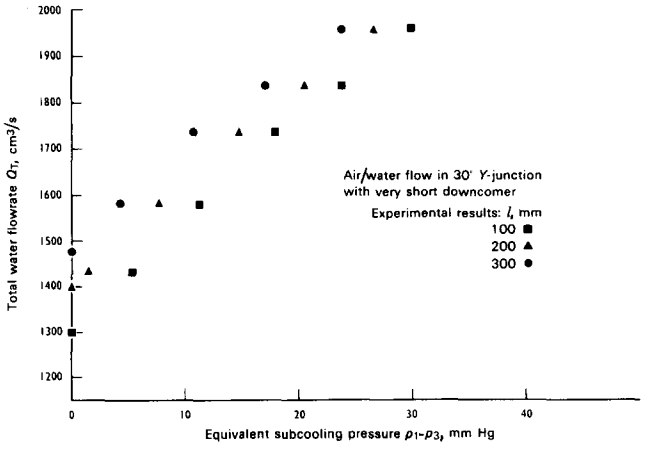

Fig. 6. Flooding of 30° Y-junction with a very short downcomer with air–water flow: effect of simulated subcooling pressure p_1-p_3

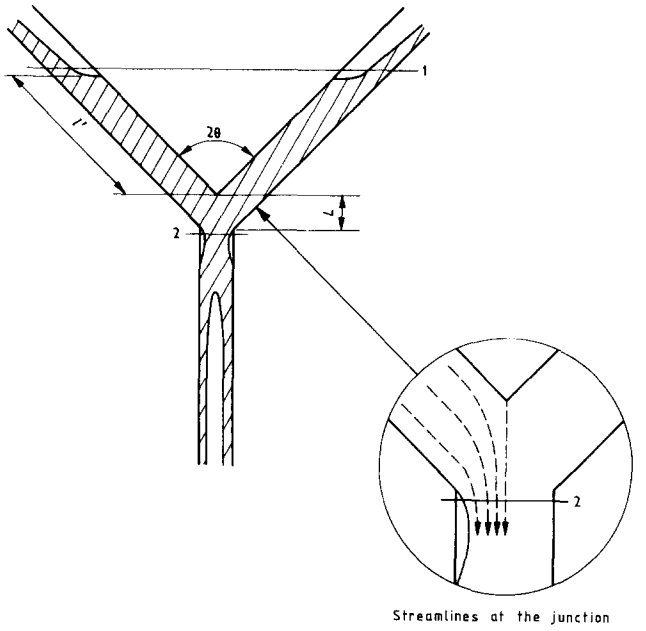

Fig. 7. System considered in the development of the model

The momentum equation between stations 1 and 2 can be written for the vertical direction as

$$M_1 + P_1 + G + D = M_2 + P_2 \tag{1}$$

Neglecting the contribution of steam, the vertical component of the inlet momentum is

$$M_1 = 2\rho_w V_{1w}^2 A_{1w} \cos\theta \tag{2}$$

The vertical component of the outlet momentum is more difficult to evaluate since the streamlines at station 2 are not parallel (see insert in Fig. 7) and their direction is not easily calculated. Instead, it is assumed that for the purpose of calculating the vertical component of the momentum at station 2, the effective angle of the mean velocity there, V_{2w}, to the vertical is α_M and thus

$$M_2 = \rho_w V_{2w}^2 A_{2w} \cos^2 \alpha_M \tag{3}$$

The gravitational and the approximate vertical component of the friction force acting on the fluid are, respectively,

$$G = \rho_w g(l' \cos\theta + L)\pi R^2 \tag{4}$$

and

$$D = 2\tau_w(2\pi R l') \cos\theta \tag{5}$$

where

$$\tau_w = \tfrac{1}{2} f \rho_w V_c^2 \tag{6}$$

Finally, the contribution of the pressure forces can be expressed in terms of the head of the liquid used in the experiments (water in the present case) as

$$P_1 - P_2 = \rho_w g h \pi R^2 \tag{7}$$

The continuity equations for stations 1 and c, anywhere in the water columns, are, respectively

$$V_{1w} A_{1w} = Q_{wl} \tag{8}$$

$$V_c \pi R^2 = Q_{wl} \tag{9}$$

Similarly, as for the outlet momentum, there are difficulties in the evaluation of the volume flowrate at station 2 in terms of V_{2w} and A_{2w}, since the streamlines are not parallel there. Hence, as above, an effective angle α_V required for the volume flowrate is introduced and thus

$$V_{2w} A_{2w} \cos \alpha_V = 2Q_{wl} \tag{10}$$

It should be pointed out that the angles α_M and α_V are not, in general, identical since they are defined by two different methods of integration over the non-parallel streamlines

$$V_{2w}^2 \cos^2 \alpha_M A_{2w} = \int_{A_{2w}} (V \cos \alpha)^2 \, dA \tag{11}$$

$$V_{2w} \cos \alpha_V A_{2w} = \int_{A_{2w}} V \cos \alpha \, dA \tag{12}$$

Equation (1) can be written as

$$2V_{1w}Q_{wl} \cos \theta + gh\pi R^2 + g(l' \cos \theta + L)\pi R^2 - 2fl' \cos \theta \frac{Q_{wl}^2}{\pi R^3} = \frac{4Q_{wl}^2}{A_{2w}} \beta \tag{13}$$

Only a small error is introduced by assuming that

$$l' + \frac{L}{\cos \theta} = l \tag{14}$$

and by using l instead of l' in the fourth term on the left-hand side of eq. (13). Equation (13) thus simplifies to

$$2V_{1w}Q_{wl} \cos \theta + gh\pi R^2 + gl \cos \theta \pi R^2 - 2fl \cos \theta \frac{Q_{wl}^2}{\pi R^3} = \frac{4Q_{wl}^2}{A_2 \pi R^2} \beta \tag{15}$$

Equation (15) contains two non-primary parameters, the generalized momentum correction coefficient, β, and the dimensionless cross-sectional area, A_2. Since in the present case they occur only as a ratio whose physical meaning, as shown by eq. (18), is that of a discharge coefficient, let

$$\frac{A_2}{\beta} \cos \theta = C_d \tag{16}$$

and thus, effectively, only one non-primary parameter is required.

3.2 Application to Saturated Steam–Water Flow

In saturated flow, the steam pressure p_1 is equal to the saturation pressure of the condensate. If, furthermore, the vertical limb is unobstructed in the vicinity of the junction (as in the present state) and thus no additional head is required to discharge the liquid through the vertical limb there, steam spaces will be formed just below the junction (see Fig. 2(a)). The pressure there and thus the pressure p_2 will also be equal to the saturation pressure of the condensate and thus eq. (15) simplifies to

$$\left[1 - 2f\left\{\frac{Q_{wl}}{\pi(gR^5)^{1/2}}\right\}^2\right] \frac{l}{R} = \frac{4}{C_d}\left\{\frac{Q_{wl}}{\pi(gR^5)^{1/2}}\right\}^2 - \frac{2V_{1w}}{(gR)^{1/2}}\left\{\frac{Q_{wl}}{\pi(gR^5)^{1/2}}\right\} \tag{17}$$

Table 1(a)

Experimental values of discharge coefficients obtained with steam–water flow

	θ deg	15	30	45
$[Q_T^*]_{min}$	cm^3/s	1200	1050	900
$[Q_T^*]_{max}$	cm^3/s	1250	1150	950
$[C_d]_{min}$		0·65	0·62	0·61
$[C_d]_{max}$		0·67	0·67	0·64

As pointed out above, it is difficult to evaluate C_d theoretically, since in general it may be a complex function of several parameters and thus a different approach is used.

First, it is assumed that for $l/R \geqslant 0$, C_d is only a function of the angle θ. Since at incipient flooding, $l/R = 0$, C_d can be obtained from eq. (17) as

$$Q_T^* = C_d V_{1w}^* \pi R^2 \tag{18}$$

The total water flowrate at incipient flooding was measured and the corresponding water approach velocity was calculated from the following expression

$$\frac{V_{1w}}{(gR \cos \theta)^{1/2}} = 5{\cdot}9\left\{\frac{Q_{wl}}{(gR^5 \cos \theta)^{1/2}}\right\}^{0{\cdot}22} \tag{19}$$

which was derived by Kubie and Gardner (**2**). The discharge coefficient C_d was then calculated and its values are shown in Table 1(a).

The relative length of the water columns, l/R, for flowrates above those for the incipient flooding is calculated from eq. (17) using the above obtained values of the discharge coefficients as

$$\frac{l}{R} = \frac{\frac{4}{C_d}\left[\frac{Q_{wl}}{\{\pi(gR^5)^{1/2}\}}\right]^2 - \frac{2V_{1w}}{(gR)^{1/2}}\left[\frac{Q_{wl}}{\{\pi(gR^5)^{1/2}\}}\right]}{1 - 2f\left[\frac{Q_{wl}}{\{\pi(gR^5)^{1/2}\}}\right]^2} \tag{20}$$

To compare the present model with experimental data, the Fanning friction factor f must be known. The theoretical results are not very sensitive to its choice but the best agreement between the theoretical predictions and experimental results was obtained with $f = 0{\cdot}0035$ and this is the value used throughout. The theoretical results are compared with experimental data in Fig. 3, which shows reasonable agreement between the theory and the experiments. Hence the assumption that the discharge coefficient is independent of l and Q_{wl} seems to hold fairly well.

3.3 Application to Subcooled Water–Steam Flow

It can be seen from Fig. 4 that an increase in the water subcooling increases the apparent discharge capacity of Y-junctions. This is because subcooled water can be depressurized down to its saturation pressure and when this happens below the junction it helps to accelerate the water through it. In applying the present model to this aspect of the work it is assumed that this process is indeed taking place and that the difference in the static pressure over the length of the water columns is given by the subcooling pressure of the water. The pressure was

measured directly in the present work. Using the assumptions and approximations of sub-section 3.2 (except that h is not zero in this case), eq. (15) simplifies to

$$\frac{h}{R} = \frac{4\cos\theta}{C_d}\left|\frac{Q_{wl}}{\pi(gR^5)^{1/2}}\right|^2 - 2\cos\theta\,\frac{V_{lw}}{(gR)^{1/2}}\left|\frac{Q_{wl}}{\pi(gR^5)^{1/2}}\right| + \frac{l}{R}\cos\theta\left[2f\left|\frac{Q_{wl}}{\pi(gR^5)^{1/2}}\right|^2 - 1\right] \quad (21)$$

Hence, if the water subcooling is known, h is known too and the relationship between the flowrate and the length of the water columns may be determined.

Theoretical results of the present model, with $f = 0{\cdot}0035$, are compared with experimental data in Fig. 4 from which, once again, reasonable agreement may be observed.

The incipient flooding flowrate for subcooled water can be obtained from eq. (21) by putting l/R equal to zero. Theoretical results for the incipient flooding with subcooled water in the 30° Y-junction are included in Fig. 4. It should be noted that due to experimental difficulties no experimental data were obtained for incipient flooding with subcooling.

3.4 Modification for Air–Water Flow

As mentioned in sub-section 2.3 experiments have also been undertaken to investigate the flow of air and water in Y-junctions with very short vertical limbs. Comparison of Figs. 3 and 4 with Figs. 5 and 6, respectively, indicates that the air–water results are close to steam–water results in spite of some discernible differences. It was also noted in Section 2 that there were some differences between the two flow regimes within the water columns. In the case of steam–water flow, the steam bubbles rapidly collapsed on entry to the water columns, so that the water columns could be regarded as consisting of water only. However, in the case of air–water flow air bubbles were distributed throughout the length of the water columns and because of buoyancy forces were preferably situated near the top surfaces of the inclined limbs (see Fig. 2(b)).

It can be shown that this persistent presence of the gas phase in the water during the air–water flow modifies the governing equations by changing the effective density and the flow area available to water. However, such a simple model fails in predicting some of the differences between steam–water and air–water flow. This is probably due to more complex interactions between entrained air bubbles and the water flow.

The incipient flooding flowrates are displayed in Table 1(b).

Table 1(b)

Experimental values of discharge coefficients obtained with air–water flow

	θ deg	15	30	45
$[Q^{\ddagger}]_{min}$	cm^3/s	1250	1075	950
$[Q^{\ddagger}]_{max}$	cm^3/s	1325	1150	1000
$[C_d]_{min}$		0·67	0·63	0·62
$[C_d]_{max}$		0·69	0·67	0·65

4 DISCUSSION

4.1 Steam–Water Flow in Y-junctions

The simple model developed in Section 3 predicts results which are in reasonable agreement with experimental data, even though some differences between predictions and experiments are apparent. There are many possible reasons for the differences but it is probable that the major one is that the discharge coefficient C_d is not only a function of the angle of the Y-junction, as was assumed for the development of the model, but depends additionally, for example, on the flowrate and the length of the water column. The model could be improved by allowing the discharge coefficient to change with flowrate and the length of the water column, i.e., by fitting the model to experimental data more closely. However, the advantage of the present model is its simplicity and the fact that only one empirical constant is required for a given Y-junction, and this probably outweighs its disadvantages.

The model can be also used to predict the improvement in the apparent discharge capacity of Y-junctions when subcooled water is used. This improvement can be sometimes quite dramatic depending on the degree of water subcooling.

It can be noted that the length of the vertical limb does not enter into the arguments used for the development of the model, since the pressure just below the junction depends on the state of the water and not the length of the vertical limb.

Finally, it was observed that the Y-junction itself did not introduce any flow instabilities. Only the steam–water interfaces at the top of the water columns were sources of instabilities because of considerable steam bubble entrainment and collapse there.

4.2 Modelling with Air and Water

It has been shown in Section 2 that when air–water modelling is used in Y-junctions with very short vertical limbs, the experimental results on flooding and rise of the water level above the junction thus obtained are similar to those obtained with steam–water flow. The major difference between the two systems is in the number of gas bubbles mixed with the water phase. In the case of steam–water flow the steam bubble entrainment is low and the bubbles are localized. On the other hand, in the case of air–water flow the air bubbles are numerous and distributed throughout the length of the water columns and the downcomer and the flow is less steady.

Thus, for some preliminary investigations, the results obtained with air–water analogues may be regarded as acceptable, taking into account the considerable saving of time and effort associated with the air–water modelling. If this is to be done care must be taken to ensure that where flow separation or flashing is likely, the geometry of the air–water analogue is such that suction pressures are prevented from occurring by suitable venting arrangement, since depressurization in air–water flow does not have, in general, an equivalent in steam–work flows, where the steam would flash and prevent it from developing.

For example, the only empirical factor required in the present model is the discharge coefficient C_d. Comparison of Table 1(a) with Table 1(b) shows that the steam–water system and the air–water system with a short vertical limb give, for identical values of the Y-junction angle, θ, similar values of the flooding flowrates and the discharge coefficients, C_d. This thus suggests the air–water system may be used with confidence to obtain the required empirical parameters also for other configurations.

4.3 Implication for Design

As pointed out above the steam–water interfaces at the top of the water columns in flooded Y-junctions are sources of large scale steam entrainment and associated instabilities. Hence flooding of a Y-junction has a major influence on its operation and thus certain design criteria for its control are discussed below.

The general condition of incipient flooding of a Y-junction with saturated steam–water flow is given by eq. (18). In order to use eq. (18) the approach water velocity must be determined from the geometry of the junction and the energy or the momentum equations. Using this velocity the incipient flooding flowrate is then calculated. For flowrates greater than the incipient flooding flowrate the junction will be flooded.

The numerical values of the discharge coefficient, C_d, are between 0·7 and 0·6 for the junctions investigated in the present work and are decreasing with increasing angles of the junction. It is interesting to note that for a true orifice outflow from a large tank through a sharp circular outlet the discharge coefficient is about 0·6, which might be the asymptotic value of C_d for θ approaching 90°. It should also be noted that for θ approaching zero the discharge coefficient should tend to unity. However, it would be unwise to extrapolate the results beyond the range of Y-junction angles investigated in the present work.

The implication of eq. (18) is that the angle θ has only a small direct influence on the incipient flooding flowrates. The major influence on flooding flowrates is due to the cross-sectional area and the approach velocity. If the approach velocity is independent of θ, the incipient flooding flowrate will increase only marginally with the decreasing angle of the junction. However, it should be pointed out that in some cases the approach velocity increases considerably with decreasing angle of the junction and the incipient flooding flowrate can thus increase substantially too. Hence, it is always beneficial to decrease the angle of the junction if it is required to increase the incipient flooding flowrates. The design of the pipework downstream of the junction does not influence its discharge capacity, provided that the flow resistances downstream of the junction are sufficiently small for their effect not to propagate back to the junction.

5 CONCLUSIONS

Steam–water flows through Y-junctions have been investigated. It has been shown that, at low water flowrates, water falls freely through the junction. However, as the water flowrate increases, a condition is reached at which water starts to pile up at the junction and the junction is said to be flooded. Further increase in the water flowrate causes the water level to rise within the sloping limbs approaching the junction. It has been also shown that as the subcooling of the water increases, the apparent discharge capacity of the junction and the flowrates required for flooding increase too.

A simple theoretical model has been developed which describes reasonably well the flow phenomena observed.

It has also been demonstrated that in some circumstances air–water modelling gives acceptable representation of steam–water flows in Y-junctions.

Finally, design criteria have been developed for controlling flooding in Y-junctions with steam–water flow.

ACKNOWLEDGEMENT

This work was carried out at the Central Electricity Research Laboratories and is published by permission of the Central Electricity Generating Board.

REFERENCES

(1) SIMPSON, L. L. 'Sizing piping for process plants', *Chem. Eng.* 1968, **75** (13), 192

(2) KUBIE, J. and GARDNER, G. C. 'Two-phase gas–liquid flow through Y-junctions', *Chem. Engng. Sci.* 1978, **33**, 319